

Lawrence Berkeley National Laboratory

Recent Work

Title

Statistical analysis of the Nb3Sn strand production for the ITER toroidal field coils

Permalink

<https://escholarship.org/uc/item/4d279223>

Journal

Superconductor Science and Technology, 30(4)

ISSN

0953-2048

Authors

Vostner, A
Jewell, M
Pong, I
[et al.](#)

Publication Date

2017-02-20

DOI

10.1088/1361-6668/aa5954

Peer reviewed

PAPER

Statistical analysis of the Nb₃Sn strand production for the ITER toroidal field coils

To cite this article: A Vostner *et al* 2017 *Supercond. Sci. Technol.* **30** 045004

View the [article online](#) for updates and enhancements.

Related content

- [Challenges and status of ITER conductor production](#)
A Devred, I Backbier, D Bessette *et al.*
- [Performance analysis of the toroidal field ITER production conductors](#)
M Breschi, D Macioce and A Devred
- [Technology development and mass production of Nb₃Sn conductors for ITER toroidal field coils in Japan](#)
Y. Takahashi, T. Isono, K. Hamada *et al.*

Recent citations

- [Properties of Toroidal Field Nb₃Sn Strands Made for the ITER Chinese Domestic Agency](#)
Fang Liu *et al*
- [More time for Nb₃Sn magnet conductors](#)
Lance D Cooley



IOP | ebooks™

Bringing you innovative digital publishing with leading voices to create your essential collection of books in STEM research.

Start exploring the collection - download the first chapter of every title for free.

Statistical analysis of the Nb₃Sn strand production for the ITER toroidal field coils

A Vostner¹, M Jewell², I Pong³, N Sullivan², A Devred¹, D Bessette¹,
G Bevilard¹, N Mitchell¹, G Romano¹ and C Zhou¹

¹ ITER Organization, Route de Vinon-sur-Verdon, CS 90 046, F-13067 St. Paul Lez Durance Cedex, France

² Materials Science Program, University of Wisconsin-Eau Claire, Eau Claire, WI 54702, United States of America

³ Accelerator Technology and Applied Physics Division, Lawrence Berkeley National Laboratory, Berkeley, CA 94720-8201, United States of America

E-mail: alexander.vostner@iter.org

Received 27 September 2016, revised 20 December 2016

Accepted for publication 13 January 2017

Published 20 February 2017



CrossMark

Abstract

The ITER toroidal field (TF) strand procurement initiated the largest Nb₃Sn superconducting strand production hitherto. The industrial-scale production started in Japan in 2008 and finished in summer 2015. Six ITER partners (so-called Domestic Agencies, or DAs) are in charge of the procurement and involved eight different strand suppliers all over the world, of which four are using the bronze route (BR) process and four the internal-tin (IT) process. In total more than 500 tons have been produced including excess material covering losses during the conductor manufacturing process, in particular the cabling. The procurement is based on a functional specification where the main strand requirements like critical current, hysteresis losses, Cu ratio and residual resistance ratio are specified but not the strand production process or layout. This paper presents the analysis on the data acquired during the quality control (QC) process that was carried out to ensure the same conductor performance requirements are met by the different strand suppliers regardless of strand design. The strand QC is based on 100% billet testing and on applying statistical process control (SPC) limits. Throughout the production, samples adjacent to the strand pieces tested by the suppliers are cross-checked ('verified') by their respective DAs reference labs. The level of verification was lowered from 100% at the beginning of the procurement progressively to approximately 25% during the final phase of production. Based on the complete dataset of the TF strand production, an analysis of the SPC limits of the critical strand parameters is made and the related process capability indices are calculated. In view of the large-scale production and costs, key manufacturing parameters such as billet yield, number of breakages and piece-length distribution are also discussed. The results are compared among all the strand suppliers, focusing on the difference between BR and IT processes. Following the completion of the largest Nb₃Sn strand production, our experience gained from monitoring the execution of the QC activities and from auditing the results from the measurements is summarised for future superconducting strand material procurement activities.

Keywords: ITER, Nb₃Sn strand, critical current, strand performance, production

(Some figures may appear in colour only in the online journal)

1. Introduction

The superconducting magnet systems of ITER include a Nb₃Sn-based conductor in the toroidal field (TF) coils and

the central solenoid (CS) modules, and a NbTi-based conductor in the poloidal field coils, correction coils and feeder busbars [1, 2]. The supply of the ITER components and their specifications are defined through procurement arrangements

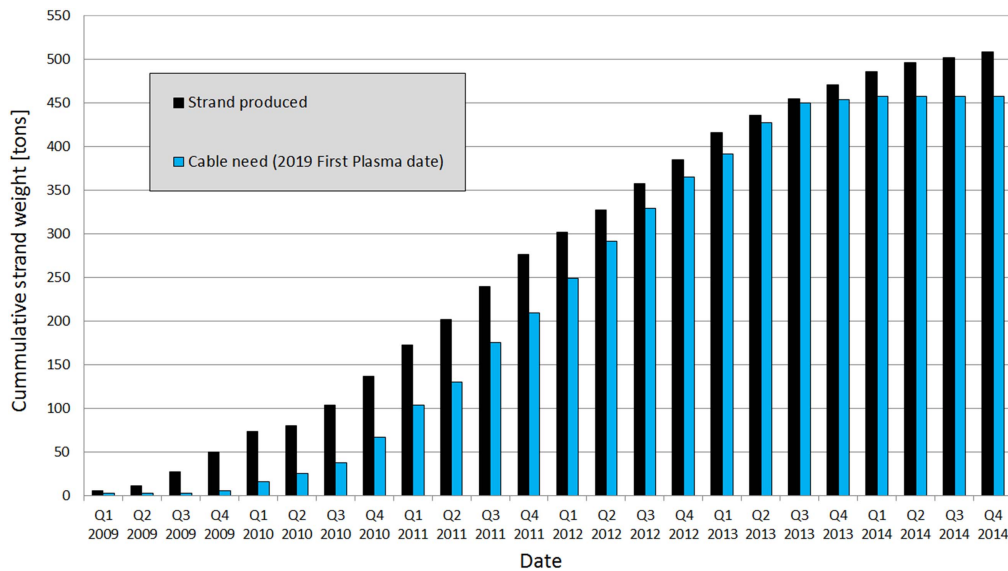


Figure 1. TF strand production dashboard for all eight suppliers. The material amount given is the brute quantity produced in the frame of the ITER TF conductors including losses during production, back up material, etc. Note that about 1–2 ton of additional material has been added in summer 2015 which is not shown here.

(so-called PAs). For the TF strand, six ITER partners—the domestic agencies (DAs)—are involved: People’s Republic of China, Europe, Japan, Republic of Korea, Russian Federation and the United States. Given the functional specification of the strand and domestic procurement policies, eight different strand suppliers are contributing to the TF conductors. Before the start of the main ITER strand production several R&D programmes [3–9] were launched all over the world to explore specification requirements suitable for ITER large scale production. Based on the outcome, the main parameters were defined, in particular the minimum acceptable critical current I_c (see section 2.3 below).

The actual TF strand production, started first in Japan in 2008, has now been completed. The production itself is split into a few phases, namely, qualification phase, pre-production and production phase, to ensure proper monitoring of performance by defining process parameter limits for each phase.

An overview of the cumulated TF strand production by time is given in figure 1. More details on the strand production at the DAs can be found in e.g. [10–14]. As it can be seen a peak production rate of 15 t month^{-1} was achieved which is about one order of magnitude more than before the ITER project. The total amount produced and registered into the database exceeds 500 tons which is significantly more than the nominal 384 tons needed for the TF conductors [15]. The excess material covers losses caused during cabling preparation (so called cable mapping where the strands and sub-stage cables are being selected) and cable/conductor archival samples required for quality control (QC) purposes. The amount of material lost during cabling depends strongly on the single piece-lengths provided by the strand supplier (see below). The average per final cable as used for the conductor is varying between 8%–25%. The archival and destructive examination samples are contributing a couple of percent. In addition, several tons have been produced as backup in

order that additional cables can be quickly produced if needed. The production rate in figure 1 is compared to the need dates for cabling based on ITER First Plasma date in 2019 to show that the TF strand production met the original schedule requirements.

2. TF strand analysis

2.1. Strand specification

Like all ITER strand specifications, the TF strand requirements are based on a functional specification where all critical strand parameters, but not the exact strand layout itself, are defined. Potential suppliers could therefore propose their preferred strand design. Some of the parameters (such as diameter) are bounded on both sides, whereas some only have a maximum (such as hysteresis loss) or minimum (such as critical current and residual resistance ratio) requirement, allowing a lot of room for design compromises. While for each supplier the production stability throughout is monitored by statistical process control (SPC), across suppliers the performance variation in some parameters can have significant systematic differences. Although the strand suppliers enjoy considerable freedom in the final strand architecture, simply meeting the strand specifications is not a sufficient condition to be qualified: the final qualification of the strand type/layout is made through a short full-size conductor test at the Sultan facility simulating the number of electromagnetic cycles in operation [16]. For the TF coils, it is not the single strand but the final conductor performance where 900 superconducting and 522 Cu strands are cabled together that is essential. Following several R&D programmes it turns out that for a given strand layout, cable/conductor parameters like sub-cable twist pitch and petal void fraction impact significantly the conductor performance and therefore, one

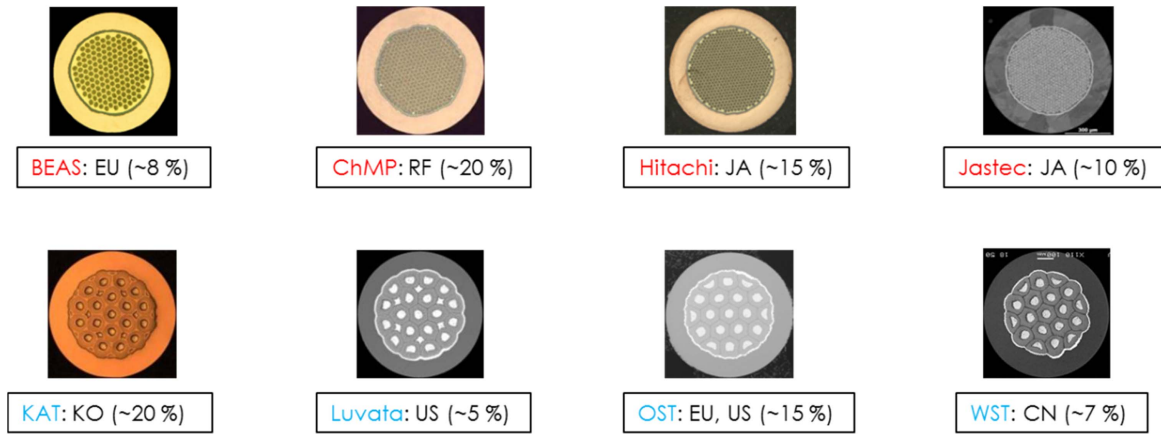


Figure 2. Cross sections of all TF strand layouts and to which DA the material is supplied. In brackets the approximate share to the TF strand production is given. The BR suppliers are Bruker European Advanced Superconductors (BEAS), Chepetsky Mechanical Plant (ChMP), SH Copper (former Hitachi Cable) and Japan Superconductor Technology (Jastec). The IT suppliers are Kiswire Advanced Technology (KAT), Luvata, Oxford Superconducting Technology (OST) and Western Superconducting Technology (WST).

Table 1. TF Strand specification and actual achieved values.

	Specification	Data (bronze)	Data (internal tin)
Outer diameter of the strand	$0.82 \text{ mm} \pm 5 \mu\text{m}$	$0.82 \text{ mm} \pm 5 \mu\text{m}$	$0.82 \text{ mm} \pm 5 \mu\text{m}$
Strand twist pitch	$15 \pm 2 \text{ mm}$	$15 \pm 2 \text{ mm}$	$15 \pm 2 \text{ mm}$
Hard Cr-coating	$2 + 0/-1 \mu\text{m}$	$2 + 0/-1 \mu\text{m}$	$2 + 0/-1 \mu\text{m}$
Critical current (at 12 T, 4.22 K, $0.1 \mu\text{V cm}^{-1}$)	$>190 \text{ A avg. defined by CPQS}$	190–255 A	240–315 A
Strand hysteresis losses on a $\pm 3 \text{ T}$ field cycle (4.22 K)	$\leq 500 \text{ kJ m}^{-3}$	40–500 kJ m^{-3}	180–600* kJ m^{-3}
n -value at 12 T and 4.2 K	>20	>20	>20
Residual resistance ratio after reaction heat treatment	>100	>100	>100
Cu/non-Cu ratio	1.0 ± 0.1	1.0 ± 0.1	1.0 ± 0.1
Piece-length (m)	>1000	up to 20 000	up to 13 000

*Upon request the upper limit of the strand hysteresis losses has been increased for some suppliers.

cannot rely on a simple strand/conductor performance correlation. This has been demonstrated in particular for the CS strand qualification [17]. The strand type/layout is qualified only if the conductor passes the conductor acceptance criterion [18]. The outcome of the DA selection and qualification process is that four bronze (BR) and four internal tin (IT) type strands with large differences in critical current (I_c) and losses were selected as the ITER TF strand. Therefore, despite the fact that all eight strand types meet the same functional requirements, their actual performance in the cable/conductor varies significantly [17]. An overview of the cross-sections of all TF strand layouts is given in figure 2.

Since the total number of qualification and conductor unit lengths requiring testing at Sultan is about 140, and that the preparation and test of each sample takes roughly three months, 100% conductor testing is not practical financially and schedule-wise. The project quality management strategy is therefore to ensure stable strand properties during production by applying tight QC and control limits. I_c (or the critical current density J_c), being the most critical parameter for conductor performance, is used for ensuring conductor performance without a full size conductor test. Once a strand layout is qualified by passing a full-size conductor test at the Sultan facility [16], the average I_c ($I_{c,avg}$) is defined by the material produced for the qualification. The lower control

limit (LSPC) for I_c is defined by $(I_{c,avg} - 3\sigma)$ where σ is the standard deviation from the strand material produced for the conductor qualification sample. Following previous ITER strand pre-qualification activities [3–9] a lower specification limit (LCL) for I_c has been applied with 190 A, and suppliers are required to meet the higher of the two limits. Table 1 summarises the main strand requirements for the ITER TF conductors compared to the actual performance achieved by the BR and IT strands. As indicated in table 1 most strand types comfortably exceed the minimum I_c requirement and should be considered for future large scale productions.

2.2. Production yield and piece-lengths

Due to the tight project schedule requirements, the strand suppliers had to significantly scale-up their capacity of Nb_3Sn production. Some strand suppliers managed to produce up to 3.5 t month^{-1} , where high billet yield and low numbers of breakages were crucial in achieving such a high production rate. Accordingly, these parameters are the main indicators of the level of maturity of a production process. Figure 3 shows the yield development and the number of breakages per billet of two selected BR suppliers with comparable final billet sizes of around 100 kg. As with all forthcoming plots in this paper, the billet numbers/counts are practically representative for

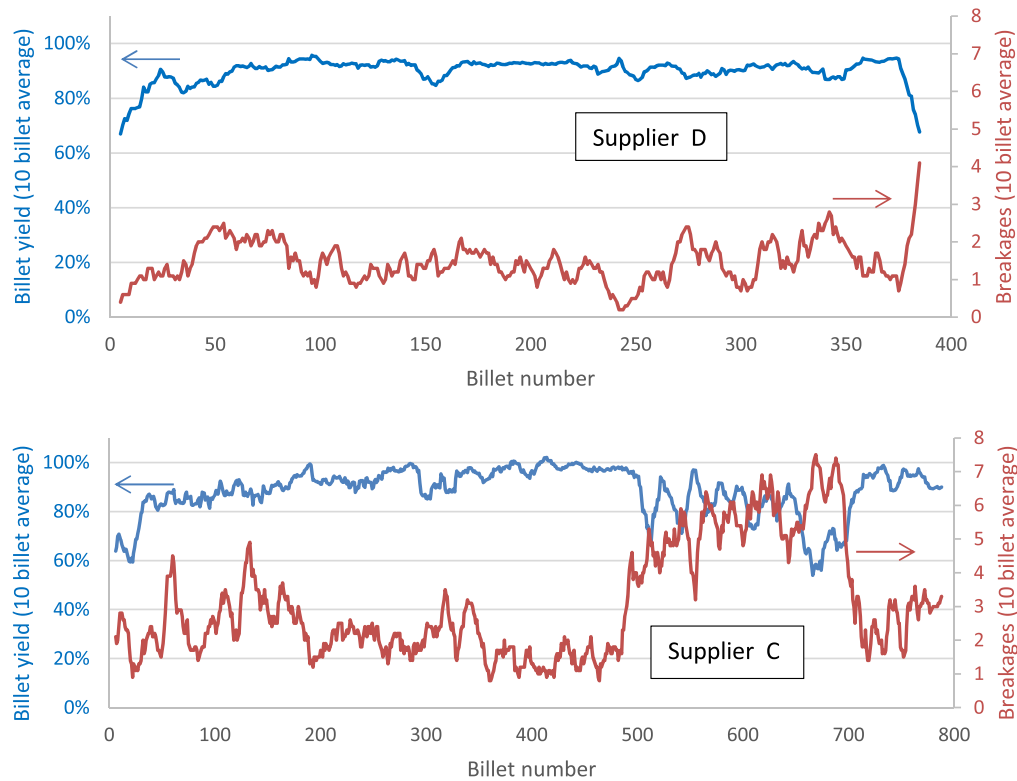


Figure 3. Billet yield development with production time for two selected BR suppliers.

the production sequence in time, i.e. billet 1 was produced first. A target yield of $\sim 100\%$ is defined as the maximum piece-length that can be delivered as final product (as determined during qualification, see discussion on yield below) and is not based on the material weight of the assembled restack billet before extrusion or drawing. This enables a better comparison between the different assembly and layout designs. Due to the different strand design and manufacturing parameters, the billet sizes among suppliers vary significantly from 40 up to 170 kg (net weight of final strand piece-lengths).

As expected, for some suppliers a ramp up in yield has been observed in the beginning which is related to the scale up of production. The first batches of billets—equivalent to an amount up to some tons—are part of the process qualification phase. This material was used for conductors foreseen for trials but not for the final magnets. Comparing the two suppliers in figure 3 it can be seen that both suppliers reached constant high yield after the qualification phase in the beginning. The number of breakages reduced accordingly which is noticeable in particular for Supplier C where the optimum conditions were reached around billet 400. This confirms the strand design can achieve good performance in production throughput. However, the performance changed significantly (the manufacturing process itself was unchanged) for billets 500–700 where in particular the number of breakages increased suddenly. The main cause for this was identified to be changes in factory floor layout workshop area during production. This demonstrates that if one is looking for the highest yield and performance, any modifications in the process or manufacturing environment must be well qualified

before implementation. For ITER, design or process changes are discouraged and may require re-qualification, depending on the level of modifications. However, changes of factors not directly related to the strand design or manufacturing process (e.g. different staffing) or workshop refurbishments (e.g. rearrangement of equipment, etc) cannot be covered and are up to internal supplier qualification. Here is another example showing how sensitive the manufacture of Nb_3Sn strand is even to the slightest of changes: Supplier D kept the high yield and good breakage performance throughout the production. The sudden decrease in yield and increased number of breakages for the last billets was related to the ramp down of the production.

The yield development for two IT suppliers with billet sizes around 50 kg is shown in figure 4. Although both suppliers have a constant high yield throughout the production, their breakage performances are different. While Supplier E has an average breakage level of 0.67 per billet, Supplier H reaches 1.54. Analysing the breakage performance as a function of production date, one can note periods of better performance (e.g. billet range 200–400 and 500–600) with a larger number of billets having no breakages. While the improvement around billet 200 is related to re-start of main strand production, the reasons for the increase of breakages after billet number 650 is not fully confirmed but likely due to external factors not related to the manufacturing process itself. It is to be noted that Supplier E has continuously increased the final yield over the production without changing the billet size/geometry and therefore, the target yield of 100% as defined as a reference after qualification has been exceeded by the end of production.

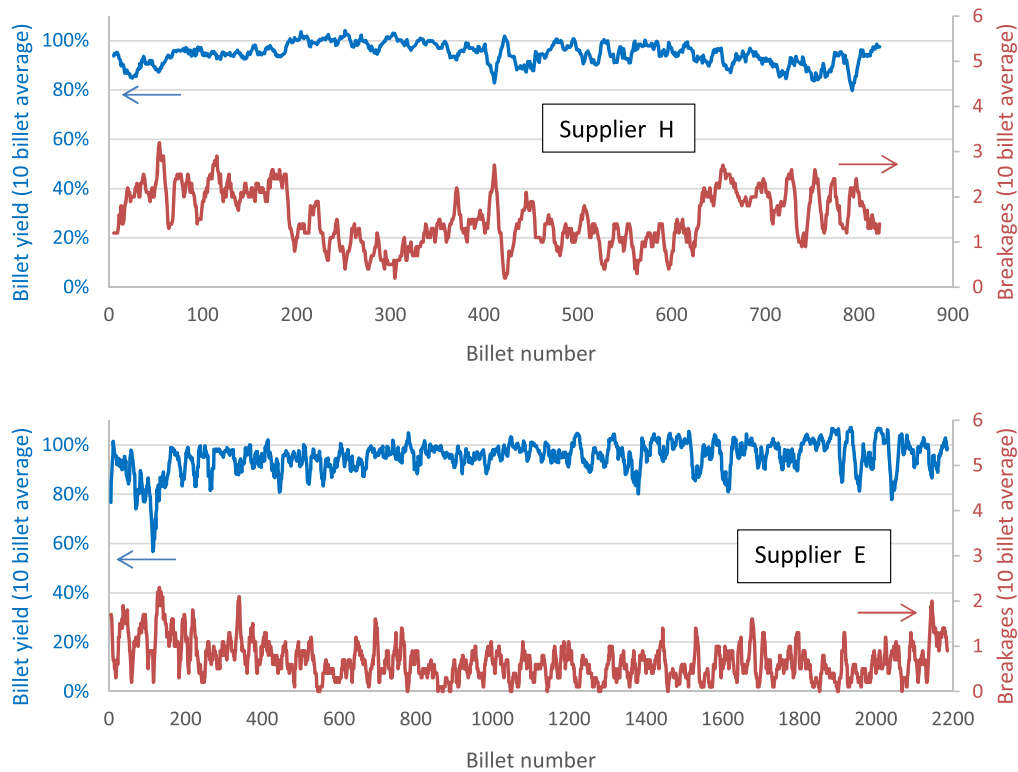


Figure 4. Billet yield development with production time for two selected IT suppliers.

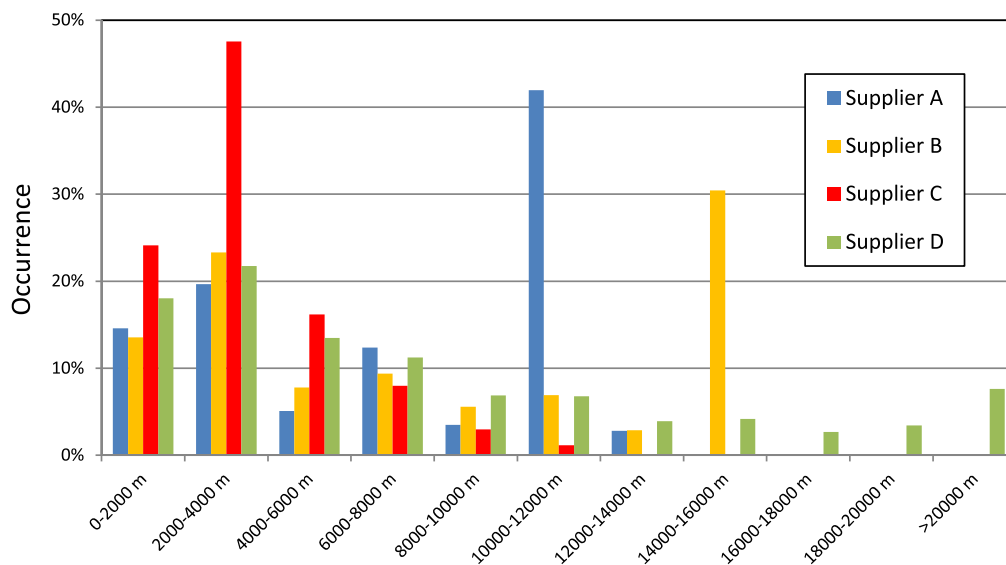


Figure 5. Piece-length distribution as a function of billet for BR suppliers.

This improvement was related to better experience of staff leading to reduced material losses during the ‘pointing’ process during drawing. Such a development has been noticed for some other IT and BR suppliers as well.

Since the ITER piece-length requirement of only 1000 m (see table 1) is not demanding, a high yield alone does not necessarily confirm a high quality process with a low number of breakages as shown in figure 4. High yield percentages can still be archived by having many short piece-lengths. Therefore, the number of piece-lengths or piece-length distribution is also an important production quality indicator. Figures 5

and 6 show histograms of piece-lengths for the BR and IT strand suppliers, respectively. All four BR suppliers (A–D) have billets without breakages. For some of them, up to 40% of the billets were drawn into a single piece-length. Given the large billet size of some strand layouts, piece-lengths are limited by the capacity of spools for transportation or the size of the drawing bench. For IT, only one supplier, Supplier G, reached a similar level of single piece-length performance (~35%) as the BR ones, and another supplier, Supplier H, has a higher population of shorter (<4 km) piece-lengths than the others.

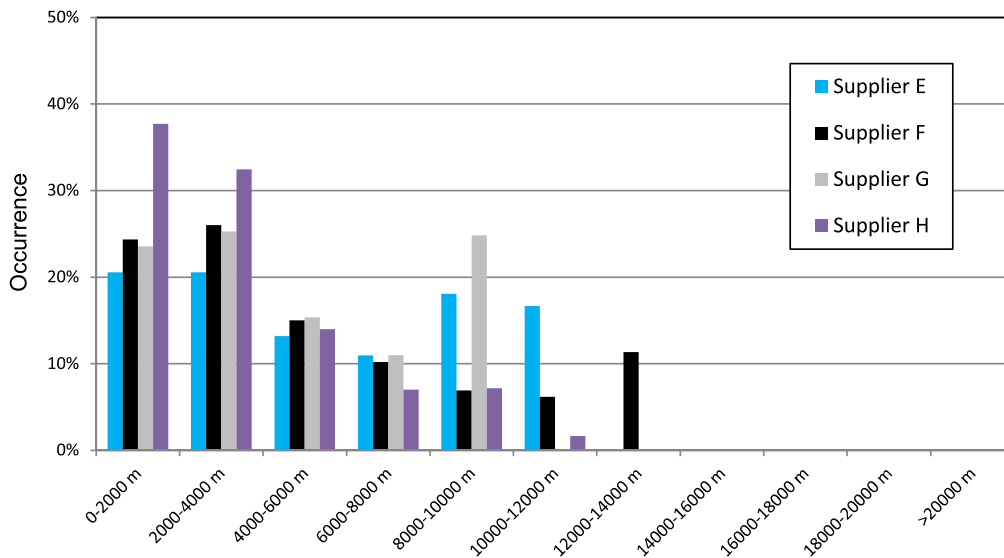


Figure 6. Piece-length distribution as a function of billet for IT suppliers.

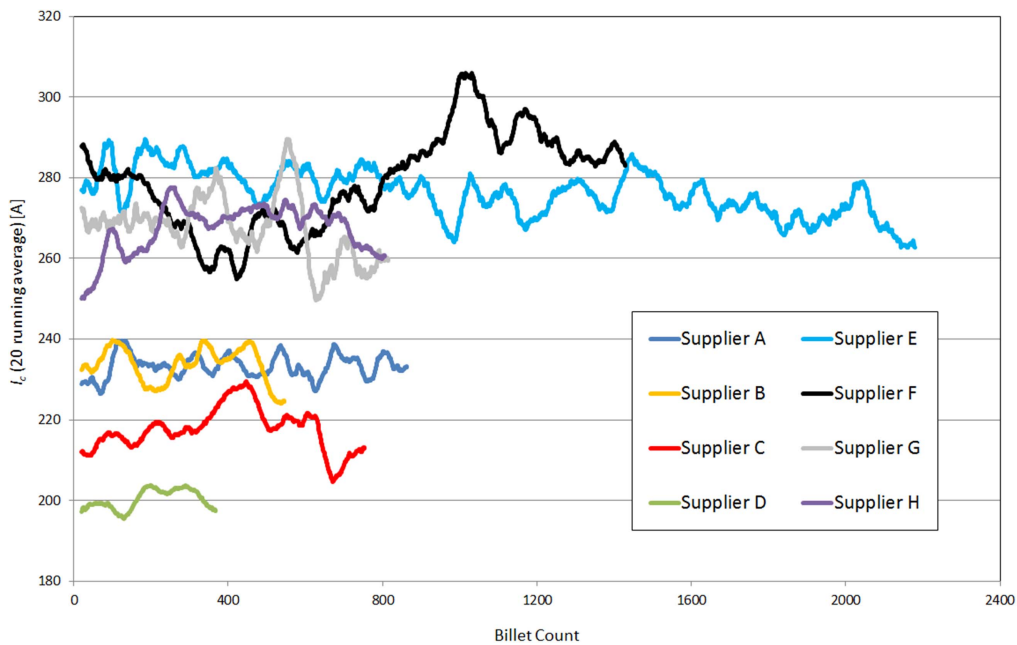


Figure 7. I_c variation for BR and IT strand supplier. Data are obtained through running average of 20 data points.

In terms of cost optimisation, the ITER strand specification did not specify a lower acceptance limit for the yield but called for investigations to understand the reason for the breakages if passing a certain threshold, which was a strategy to discourage low yield production by imposing increasing amount of investigations as penalty. Nonetheless, the ITER Organization worked with the suppliers and the DAs and agreed on a minimum billet yield of 20% during production. In the case that the yield falls below this value, those billets—even meeting the specifications—would be put aside and used only if there is no other material left. The fraction of billets with a yield of 20% or less is in the range of a few billets and this level was recorded by only some of the suppliers. Therefore, this material represents a negligible fraction of the strand production.

2.3. I_c and n -value

The full size conductor tests confirmed that, in general, strands with higher I_c provide higher critical current sharing temperatures (T_{cs}) of the conductor in particular for IT strands. Therefore, the monitoring of the strand I_c is a critical item of quality assurance. In figure 7 I_c as a function of billet ID is given for the BR and IT strand suppliers. For each billet, at least 2 I_c values (one taken from the point end and one from the tail end of the billet) are available. I_c is presented on a linear scale averaged over 20 values to provide better visibility of trends. In general, the IT I_c values are superior to the BR ones but the variation is more pronounced. While the BR suppliers' statistical control limits ($\pm 3\sigma$) typically stay within $\pm 10\%$, the IT strand types reach about $\pm 15\%$ in the best/

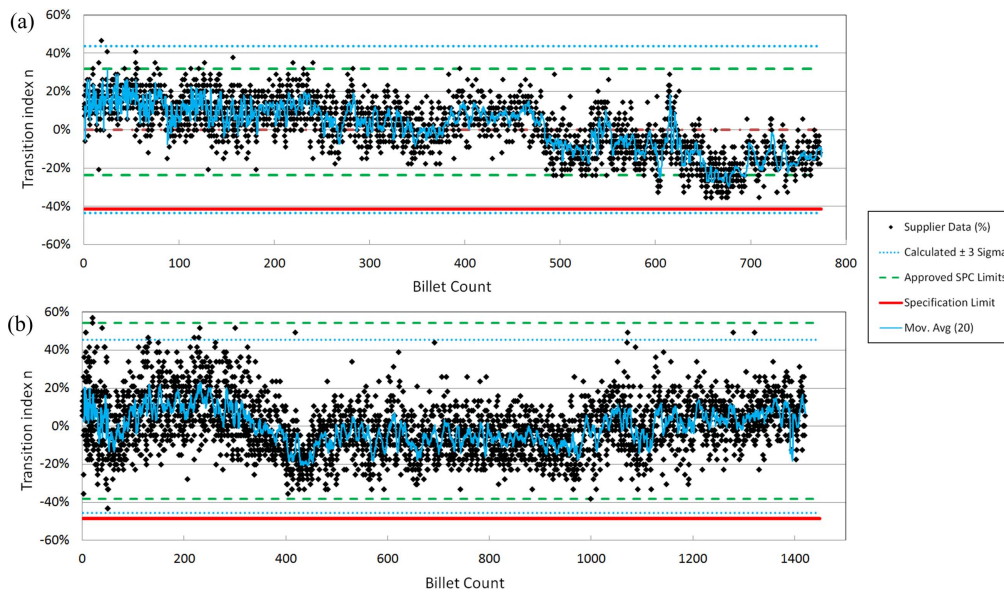


Figure 8. n -value variation for Supplier C (a) and Supplier F (b). The average values are comparable (34 and 39 for Suppliers C and F, respectively).

lowest case (a more quantitative analysis is given in the section process capability below). Furthermore, all IT strand types show long range trends and/or ‘batch-behaviours’ which are observed for other parameters as well (see below). However, within a production lot or batch the variations stay comparable to BR ones (see figure 7 Supplier E) indicating a larger influence of certain raw material and/or process variations on strand performance. A batch like behaviour leads to the conclusion that certain raw material parameters, despite staying within specification, are causing this variation. It is to be noted that the Cu ratio is not observed to have an impact on the I_c trends, i.e., the up and down trends are visible in I_c as well. As addressed below in section 4 the reproducibility of measurement results has been carefully cross-checked and the relative error within one laboratory and among laboratories remains within a few percent.

The n -values of the BR strands are high and in general show less variation than IT strands (see section 3.1 below). It is remarkable that, for IT strands having the same level of I_c , the corresponding n -values can be much different, up to a factor of 2. One would assume it is due to filament bridging but as shown later neither the absolute values nor the variation of the hysteresis losses would lead to such a conclusion. In figure 8(a) an example is given of BR n -value strand data showing a downward trend at around billet ID 450. Investigation pointed to issues in the monofilament production. However, the production cycle is long, i.e., the time from assembly of the billet until the low temperature results of the final strand are available can be 6–8 months. As a consequence, a group of billets (around ID 650) went out of the approved lower SPC limit. This example shows the relevance and importance of implementing SPC in long lead time production, so that a trend indicating production issues can be investigated for early actions to be taken: it would be too late when QC data are outside the specification limits.

2.4. Hysteresis loss

Strand hysteresis loss is a good parameter to monitor overall QC and process parameters. Given the freedom provided by the specification in the strand layout, the range of hysteresis losses covers a large range from 40 up to 600 kJ m⁻³ (see table 1). All loss measurements were done on a ± 3 T loop at 4.2 K. Like for I_c measurements the round robin tests confirmed that the reproducibility within a supplier is good and the impact in the statistical analysis negligible despite the large range and different type of measurement equipment applied. Figure 9 shows hysteresis loss data of two BR strand types selected due of their specific results. The strand data on figure 9(a) has a large variation in the beginning of the production which is related to the measurement laboratory involved. However, in the course of production the variation as well as the absolute values continue to reduce. For the last production batches covering an amount of several tons, the variation is within $\pm 10\%$ which is low considering the absolute value is around 40–50 kJ m⁻³. This continuous improvement is related to further reduction in variation of process parameters. Despite the large changes in hysteresis loss, all other QC parameters of this supplier’s strand remain stable within the variations typical for BR strand types, including I_c . Figure 9(b) represents hysteresis data more typical for the ITER TF BR strand types. Emphasised by the moving average one can observe a process related variation of around $\pm 5\%$ (i.e. ± 20 kJ m⁻³) superimposed with a ‘long range’ variation of $\pm 10\%$ related to raw materials such as observed for I_c (see above). Such a behaviour has been observed in other suppliers as well, although the material related variations are not always the same.

In figure 10 hysteresis loss data of two IT strand types are presented. Although the strand layout, billet size and final heat treatment are almost identical, the loss data are noticeably different. In the case shown in figure 10(a) the overall

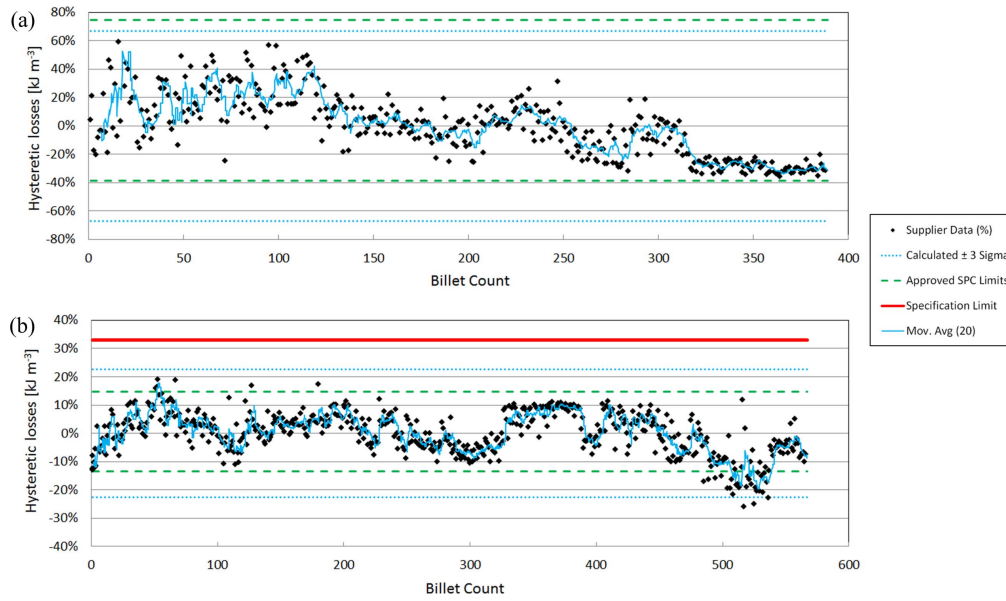


Figure 9. Hysteresis loss variation for two BR suppliers (a) D and (b) B. The average value in (a) is with 65 kJ m^{-3} much lower compared to the data shown in (b) with an average value of 376 kJ m^{-3} . The billet sizes are about 100 kg (a) and 160 kg (b). Note the scale of the two graphs is not the same and the specification limit is beyond scale.

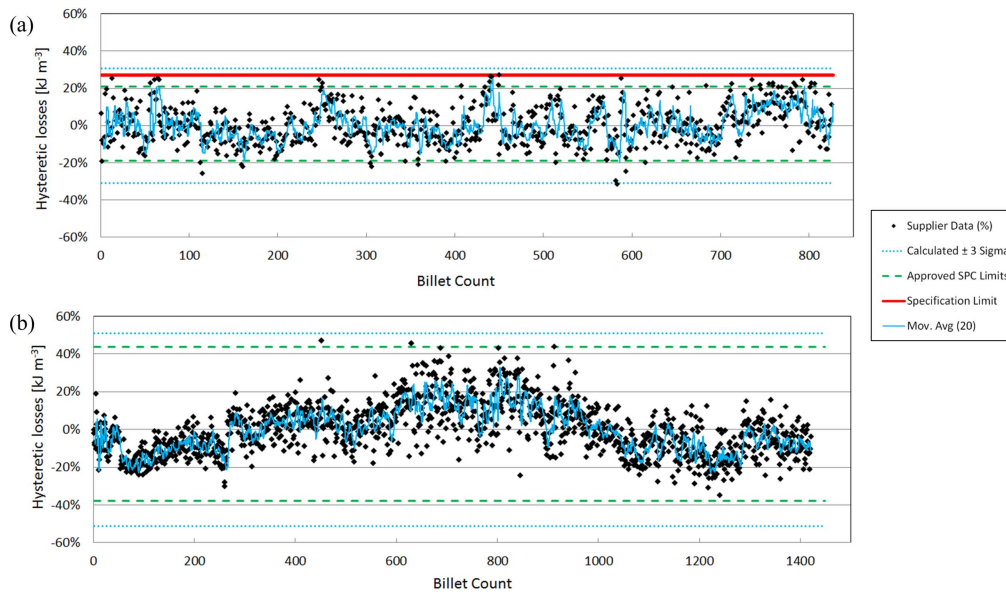


Figure 10. Hysteresis loss variation for two IT strand suppliers (a) H and (b) F. The average values of Supplier H and F are 471 and 256 kJ m^{-3} , respectively. The specification limit is out of range in (b).

variation is lower but taking into account that the average value is about twice as high as for the case shown in figure 10(b), the variation on absolute scale is comparable for both strand types. The loss data in figure 10(b) (Supplier F) shows two contributions to the total variation similar to the case for the BR strand in figure 9(b). The variation within a production batch can be as low as $\pm 10\%$. It is not as low as observed for BR strand types but very good for IT strand types, in particular considering the lower absolute value of Supplier F. As mentioned in the previous section, a general relationship between n -value and hysteresis loss could not be confirmed, e.g. the trends in figure 10(b) are not directly correlated to figure 8(b). Furthermore, low variation in losses does not mean a low n -

value variation, nor do constant losses mean high n -values. In this analysis practically all cases are observed. Detailed analyses on the relationship between the hysteresis losses and critical current density of ITER strand types are found in [19].

2.5. Residual resistance ratio (RRR) and Cr plating

The RRR values and its fluctuation strongly depend on the high temperature stages of the applied heat treatment. The 8 TF strand types are covering several different heat treatment cycles with different durations and temperature plateaux. This has to be considered if comparing the quality or RRR performance [20–22]. Furthermore, batch variations are more pronounced in case

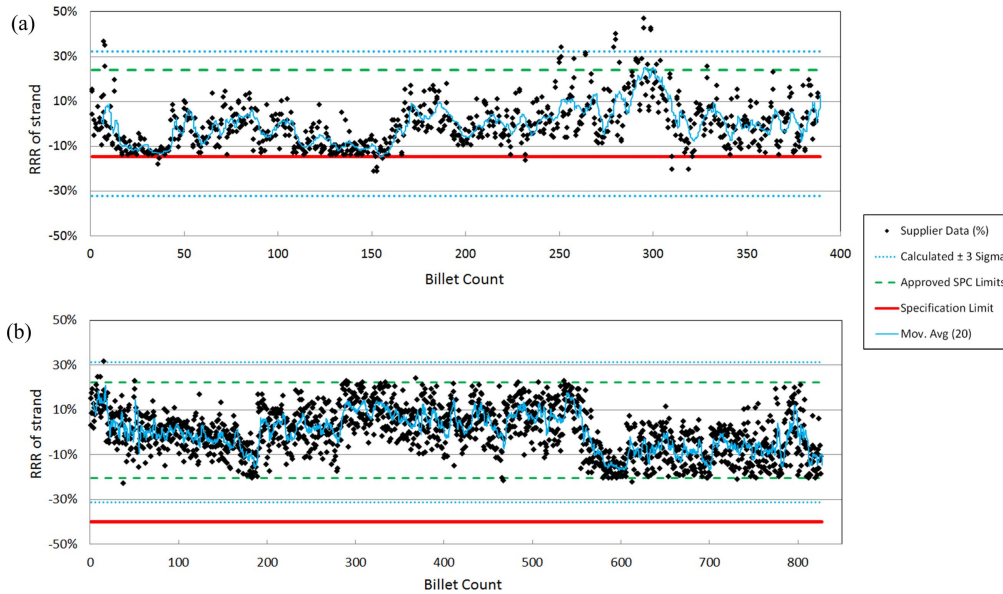


Figure 11. RRR variation for (a) bronze supplier D (average value 117) and (b) IT supplier H (average value 167).

of multiple suppliers for the Cu stabiliser. Figure 11 shows the RRR for one selected BR (a) and one IT strand type (b). The IT type as shown in this example reveals a clear batch-like behaviour (step like change around billets 200 and 550) which is related to the raw material supplier for the Cu stabiliser. All subcontracted raw material suppliers for the stabiliser met the minimum RRR requirement defined by their respective contractors (strand supplier), but the actual RRR range is raw material supplier specific and can be significantly higher than the minimum required level. The higher the RRR of the delivered Cu stabiliser, the higher is the final RRR after production and heat treatment. Such dependence is common for most suppliers but not always as clearly visible. The data in figure 11(a) have an interesting aspect. After the production of the first 100 billets a thorough analysis has been initiated by the supplier to understand the differences in RRR despite identical raw material and production processes. The responsible process step has been identified and the control parameters adapted to ensure higher RRR values, which was successful given the values shown in figure 11(a). As discussed in [17] in more detail, the RRR performance turned out to be one of the ‘unexpected’ major headaches during the ITER TF strand production calling for additional cross-check and verification tests with detailed analyses.

2.6. Cu/non-Cu ratio

As for the Cu ratio, the situation is the same for most suppliers. In order to maximise the yield, the full specification range is utilised and therefore, the approved SPC limits are set at the PA specification limits (see figure 12). This is achieved by carefully cutting the ends of the extruded or drawn bar and checking frequently the Cu ratio. After a certain supplier-specific value is obtained, the stationary zone is reached and the cropping is stopped. In the example given it can be noticed that at around billet 400 the supplier re-defined threshold level in order not to be too close to the specification limit risking non-conforming material. Suppliers D and G

have tightened their specification towards the lower end of the specification in order to maximise I_c .

2.7. Twist pitch, Cr plating thickness and diameter

For the twist pitch all the suppliers use dedicated machines with fixed settings. The required sampling rate is one measurement per piece-length. A similar situation is found for the before plating diameter which is well controlled by the last drawing die sequence. The variations observed are driven by the die refurbishment schedules of the supplier but the variations are well within specification.

The Cr plating process by contrast does require active process control. The sampling rate is defined as one measurement at the start and end of every plating process. Depending on the internal procedures of the supplier one process can cover several piece-lengths. Figure 13 provides an example for a BR strand where active control of process parameters like plating current, speed and Cr concentration in the solution is applied to keep the values within the SPC limits.

3. Process capability

3.1. Coefficient of variation

In this section the data from the TF strand suppliers are analysed in more detail through the coefficient of variation, a parameter describing the production process stability. It is derived as follows:

$$C_{\%} = \frac{\sigma}{\bar{x}}, \quad (1)$$

where σ is the standard deviation and \bar{x} the arithmetic mean of a certain parameter. A comparison of $C_{\%}$ of all suppliers is given in table 2 for the most critical strand parameters. The

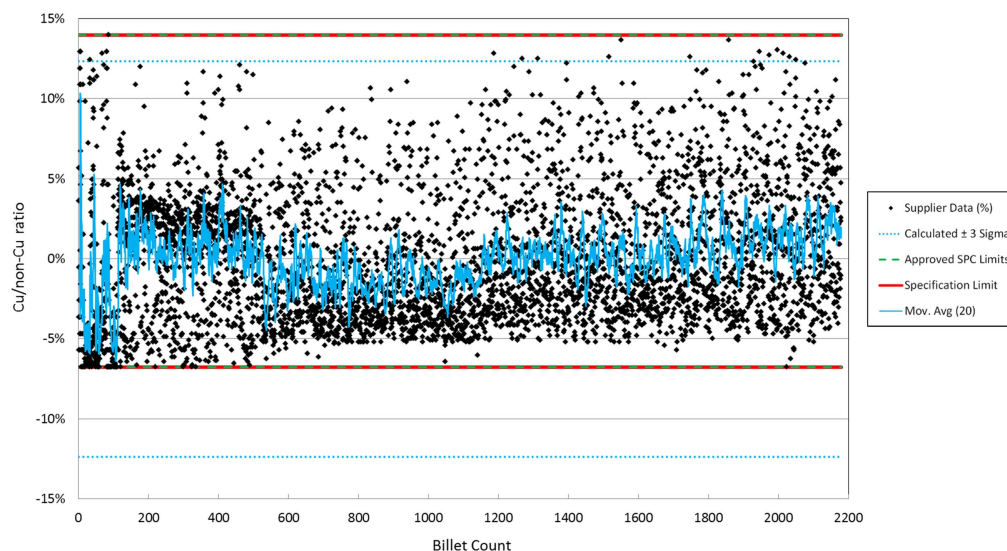


Figure 12. Cu ratio variation as a function of billet number for IT strand supplier E. Note that the QC data shown is based on the Cr plated strand, i.e., the Cr layer is considered in the Cu ratio. For this supplier, the average value of the Cu ratio is 0.96.

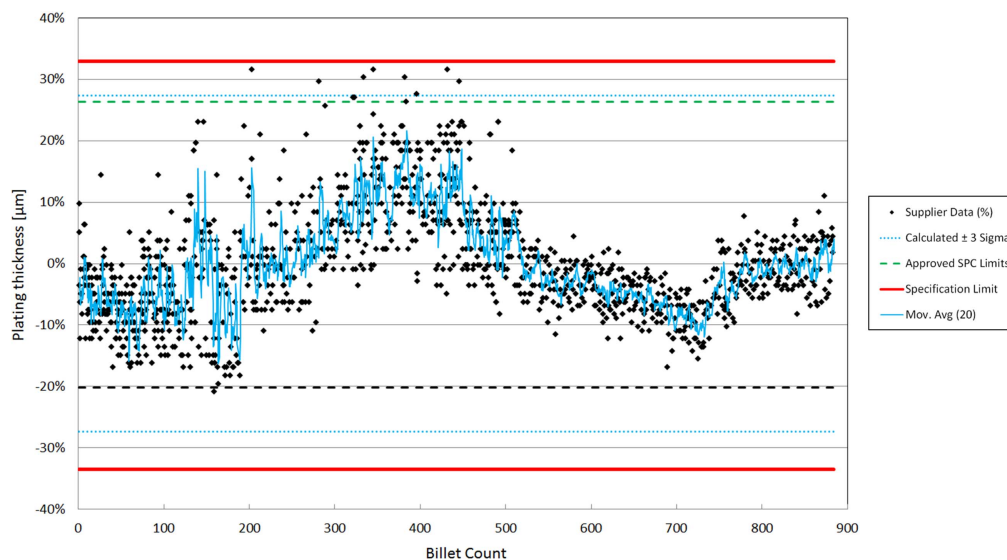


Figure 13. Cr plating thickness variation for BR supplier A. The average value is 1.5 μm .

Table 2. Coefficient of variation for selected strand parameters (in percent).

Process	Supplier	Critical current I_c	n -value	Hysteresis loss	RRR	Cu ratio	Twist pitch	Cr plating	Diameter before plating
Bronze	A	3.4	4.9	6.8	14.7	3.9	1.1	9.1	0.14
	B	3.4	6.7	7.5	13.6	3.0	3.0	7.1	0.13
	C	3.9	14.5	5.1	14.0	3.9	5.0	7.5	0.15
	D	2.1	4.1	22.3	10.7	2.5	6.3	13.8	0.15
IT	E	4.8	13.6	21.3	16.0	4.1	3.9	5.9	0.03
	F	6.4	14.6	17.0	20.7	5.3	5.4	12.2	0.13
	G	6.9	11.2	18.2	21.4	1.7	4.4	13.4	0.05
	H	4.2	7.3	10.3	10.4	4.2	2.0	3.4	0.06

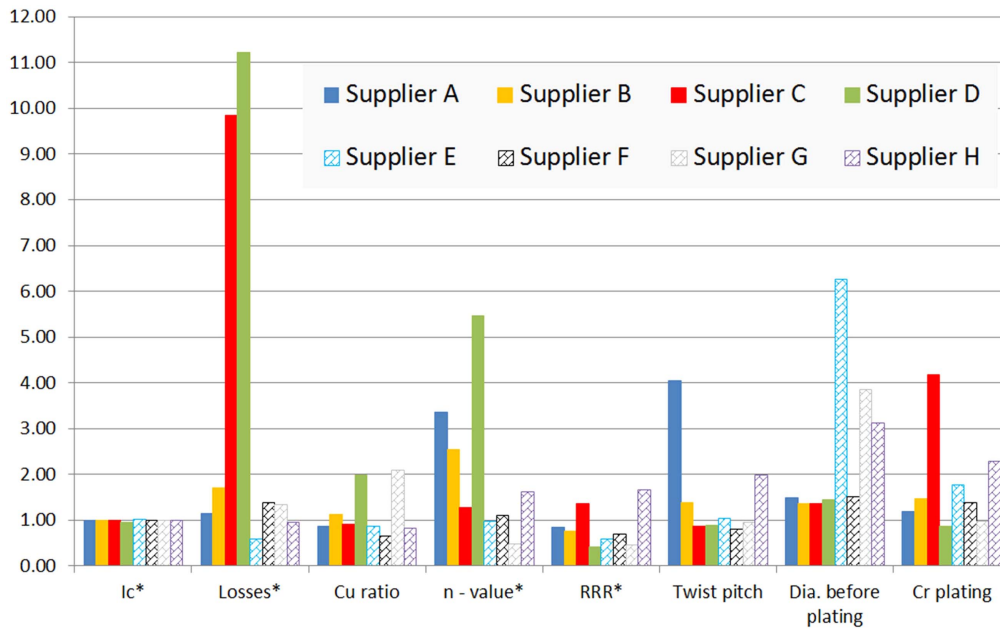


Figure 14. Process capability indices for the main strand parameters for all eight TF strand suppliers. Suppliers A–D are the BR and E–F the IT suppliers, respectively. The “*” indicates unilateral c_{pk} .

analysis reflects quantitatively what has already been discussed in section 2.3 above. I_c , n -value and hysteresis losses have a lower coefficient of variation for BR strands, in particular the losses. It has to be noted that the non-typical high variation for Supplier D is mainly due to low absolute values and due to large variations observed in the beginning of production (see figure 9(a) and section 2.4 above). If one only considers the last 20% of billets produced, the $C_{\%}$ for the losses would become 5.3%, which is in good agreement with all the other BR suppliers. Supplier C does show an unusually high variation of the n -value which is not related to the I_c or hysteresis loss performance. This is related to the peculiar filament structure of this strand design. Comparing IT strand types of the Suppliers E and H, both show high hysteresis loss leading to an increase of the acceptance limit to 600 kJ m^{-3} . The difference is that Supplier E had data covering a wide band (factor 2–3) throughout the production phases (further details see [11]), while Supplier H's data remained at a higher level but with less variation (see figure 10(a)).

Concerning RRR a slightly smaller coefficient of variation can be seen for BR which can be partly related to lower absolute values due to longer high temperature stages of their reaction heat treatment. For the Cu ratio and twist pitch, there are no distinct differences between BR and IT strand types. There are two suppliers (D and G) which have particularly low $C_{\%}$ for the Cu ratio which is coming from tighter upper limits applied by the suppliers themselves to maximise I_c . The twist pitch measurement and resolution depend strongly on the applied method and reported accuracy. Therefore, some high coefficients of variation are artefacts.

For the Cr plating, there is no direct relationship to the strand production process which is confirmed as strand suppliers using the same subcontractor for Cr plating have the same $C_{\%}$.

The (non-heat treated) diameter is found to be better controlled by the IT process because of the lack of intermediate annealing cycles which is required for the BR process.

3.2. Process capability index

To define the ability of a certain process to produce components or items, the process capability index ‘ c_{pk} ’ is commonly used in industry (a comprehensive list of references on this topic can be found e.g. in [23]). It is defined by the ratio of between the specification and control limits:

$$c_{pk} = \frac{UCL - LCL}{USPC - LSPC}. \quad (2)$$

UCL and LCL are the upper and lower CLs while USPC and LSPC are the upper and lower SPC limits defined by $\pm 3\sigma$ (the standard deviation). In case there is only one limit specified, a so-called unilateral c_{pk} is defined as:

$$c_{pk} = \frac{2(CL - \bar{x})}{\Delta SPC}, \quad (3)$$

where \bar{x} is the average value and CL either the upper or lower CL. In general a well-controlled process has c_{pk} values above 1. The process capability indices for the main strand parameter are given in figure 14. Given the way I_c specification is defined (see section 2.3 above), the expected c_{pk} is close to 1. As explained above, c_{pk} for the Cu ratio is also close to 1 to maximise production yield, except for two suppliers (D and G) who were attempting to maximise I_c . The process capability index for RRR is poor for most suppliers except Supplier H who paid careful attention in the selection of the supplier of Cu stabiliser raw material.

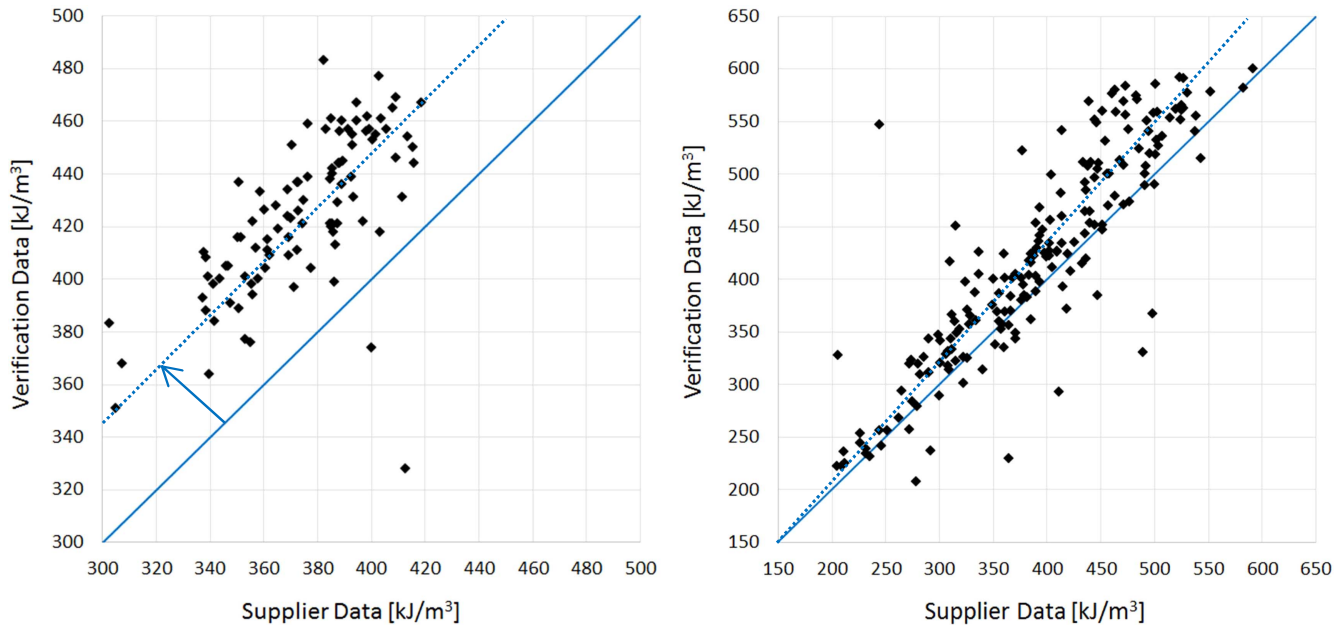


Figure 15. Comparison plot supplier versus verification lab data of hysteresis losses for Supplier B (left) and Supplier E (right). The lines are guide to the eyes only.

4. Benchmarking and cross-checking

Data used for the analysis as discussed above are based on measurements performed by the strand suppliers or sub-contracted laboratories (i.e. excluding the DA reference laboratories verification data). Given the large number of strand suppliers, a large benchmarking campaign was initiated at the start of the production to ensure measurement consistency across the board. Every laboratory involved had to pass the benchmarking using the specific test station and procedure before being qualified for performing production QC tests [24, 25]. In addition, supplier data are verified by reference laboratories nominated by the DAs. The sampling rate is defined in the PAs starting from 100% for the qualification phase down to 25% during production. Depending on the quality and consistency of the results a further reduction of the verification level is possible subject to agreement between ITER-IO and the contracting DA. These verification tests are used as a continuous cross check. In case of increased inconsistencies ITER-IO can call for further investigation. The verification samples are typically adjacent to the supplier QC sample. In figure 15 we present two examples of correlation plots of supplier data against verification data, comparing only samples from the same piece-length end to minimise the impact of local strand inhomogeneity. The ideal case is when the data population aligns along the centre diagonal line of slope = 1. A good example is given in the plot figure 15(b) with a reasonable correlation between supplier and verification data. A small tendency to higher verification data is visible but such a deviation is acceptable considering the general experimental uncertainty of hysteresis loss measurements, in particular over such a large range of absolute values. In the example give on

figure 15(a) by contrast, we can observe a systematic shift of all data where the supplier measured data are always about 50 kJ m^{-3} lower in comparison to the verification data. This triggered a cross-check campaign with the help of CERN, the ITER-IO strand reference laboratory which confirmed the verification data. Since the supplier passed the benchmarking with the reference strand, a BR type strand which had a factor of about ten lower hysteresis loss, the conclusion was that the sample preparation at the supplier is breaking some inter-filament contacts leading systematically to lower values.

During all these benchmarking and cross-checking campaigns the reproducibility and error bars of the measurements at various suppliers and laboratories have been verified as well. The self-prepared samples for the I_c measurements showed a coefficient of variation of less than 4% for the higher current internal-tin benchmarking strand [25] considering all participating laboratories. For the bronze reference strand, the coefficient of variation was only half as large. $C_{\%}$ for the hysteresis losses is higher than that for the critical current measurements but stays below 10% which is remarkable considering that the 2 benchmarking strand covered a large range from $50\text{--}2200 \text{ kJ m}^{-3}$ [25]. However, important for the strand analysis is the reproducibility within the same laboratory which is even better as it excludes systematic differences due to measurement method or sample geometry. The n -value measurements showed larger error bars, in particular for high n -value strands leading to a larger min–max range of values obtained. For this parameter, the sample preparation does play an important factor which contributes to the fact that the intra-laboratory reproducibility is much better being equivalent as found for the critical current measurements.

5. Price considerations

Being the largest Nb₃Sn strand procurement ever launched, the unit prices of ITER TF strand are of particular interest. The costs of superconductors and their components have been already extensively analyzed by Cooley *et al* [26]. A quantitative assessment of the ITER Nb₃Sn strand costs is difficult because the material is provided in-kind and only limited information on the commercial aspects of the strand procurements has been disclosed. Furthermore, the procurement activities launched worldwide were not started at the same time and, therefore, currency exchange rates and raw material base prices made direct comparisons difficult. Finally, not all procurements were driven solely by financial aspects but had national considerations as well. Nevertheless, the following conclusions can be drawn:

- A few contract prices have been published showing a price-range around €600–700 (as of 2009) per kg of final strand [27, 28] with BR being ~10% less expensive compared to IT strand types.
- Some BR strand procurements achieved unit prices around €400 per kg. Interestingly suppliers with small and large billet sizes achieved the same price level leading to the conclusion that the billet size did not play a dominant role compared to other factors in play, at least in this case where the billet sizes differs by a factor of three to four. The strand performances were practically identical so not affecting this comparison.
- Splitting the procurement into fewer lots with sizes >10 tons and tender every lot successively led to lower prices because:
 - (1) The price of the previous lots is published.
 - (2) The suppliers can better estimate the overall production yield and number of breakages from previous lot production. Despite the low minimum piece-length requirement (see table 1), the knowledge of the number of breakages per billet is essential because the QC testing requirements are related to the number of breakages per billet.
 - (3) Currency exchange rates/raw material prices can be better estimated leading to less risk and hence lower costs. For a fixed and firm price contract of longer duration (>3 yr), this factor can be in the range of 10%–15%.

The overall reduction in price due to splitting into procurement lots can be in the range of 30%–40%.

A comparison between different DAs is difficult as specific contract clauses not required by ITER but added by the DA can have a significant impact on the price per kg. For instance, the piece-length specification in the contract can be accepting integral multiples of the ITER minimum piece-length requirements of 1000 m, which simplifies cable production but leads to higher risks/costs for the strand suppliers.

6. Conclusions

The ITER project has initiated the largest Nb₃Sn strand production the world has ever seen. Eight different suppliers and many more testing laboratories all around the world were involved in the production of more than 500 t over seven years. This called for a significant ramp up of the pre-ITER worldwide Nb₃Sn strand production with three new suppliers entering the market and paved the way for the next mega-projects such as the LHC luminosity upgrade or FCC at CERN.

Comparing the BR and IT strand performances, our data have shown that the control of I_c or J_c and the hysteresis losses is better for BR strands. The 3σ I_c variation is ~10% for BR and about ~15% for IT. The low hysteresis loss is the main advantage of the BR strands. For the other monitored strand parameters, there are no striking differences. These include yield and piece-length performance where IT strands can reach the good BR piece-length performance, limited only by the billet size. It should be noted that the three ‘young’ suppliers which have been set up for this project did well and reached process performances at the same level as the better-established strand suppliers.

BR and IT processes are competitive as can be seen from the strand layout choice between them for the TF strand. The lower unit prices achieved with BR type strands are not directly related to the billet size, at least not within the billet size range seen in the ITER TF strand procurement, which spanned from 40 to 170 kg. Considering that the cost of the BR production process is not notably lower than that of IT, the main reasons are most probably related to the raw material supply, subcontracting of manufacturing steps and general commercial aspects.

Acknowledgments

We are grateful to everyone involved in the ITER conductor communities, especially those from the six Domestic Agencies involved in the TF procurement, the contracted companies and suppliers, the supporting reference laboratories and organisations, and a number of individuals who contributed in various other capacities. We particularly treasure the collaborative spirit and positive attitude which made possible this historical achievement of a successful Nb₃Sn strand production that will no doubt be a benchmark for the future.

References

- [1] Mitchell N *et al* 2008 The ITER magnet system *IEEE Trans. Appl. Supercond.* **18** 435–40
- [2] Mitchell N, Devred A, Libeyre P, Lim B and Savary F 2012 The ITER magnets: design and construction status *IEEE Trans. Appl. Supercond.* **22** 4200809
- [3] Nunoya Y *et al* 2010 Superconducting property and strain effect study of the Nb₃Sn strands developed for ITER *IEEE Trans. Appl. Supercond.* **20** 1443–6

- [4] Park P and Kim K 2008 Status of Nb₃Sn strand development in Korea *Cryogenics* **48** 347–53
- [5] Pantsyrny V, Shikov A and Vorobieva A 2008 Nb₃Sn material development in Russia *Cryogenics* **48** 354–70
- [6] Pyon T *et al* 2007 Development of high performance Nb₃Sn conductor for fusion and accelerator applications *IEEE Trans. Appl. Supercond.* **17** 2568–71
- [7] Vostner A and Salpietro E 2006 Enhanced critical current densities in Nb₃Sn superconductors for large magnets *Supercond. Sci. Technol.* **19** S90–5
- [8] Zhou L *et al* 2007 Development of multifilamentary niobium–titanium and niobium–tin strands for the International Thermonuclear Experimental Reactor project *J. Nuclear Mater.* **362** 208–14
- [9] Parrell J *et al* 2009 Internal Tin Nb₃Sn conductors engineered for fusion and particle accelerator applications *IEEE Trans. Appl. Supercond.* **19** 2573–9
- [10] Takahashi Y *et al* 2012 Mass production of Nb₃Sn conductors for ITER toroidal field coils in Japan *IEEE Trans. Appl. Supercond.* **22** 4801904
- [11] Park P *et al* 2015 Results of mass production of internal Tin Nb₃Sn strand for ITER toroidal field coil in Korea *IEEE Trans. Appl. Supercond.* **25** 6000705
- [12] Abdukhanov I *et al* 2011 Results of investigation of 500 kg Nb₃Sn bronze strand produced in Russian Federation for ITER Project *IEEE Trans. Appl. Supercond.* **21** 2567–70
- [13] Boutboul T *et al* 2016 European Nb₃Sn superconducting strand production and characterization for ITER TF coil conductor *IEEE Trans. Appl. Supercond.* **26** 6000604
- [14] Field M B *et al* 2014 Optimizing Nb₃Sn conductors for high field applications *IEEE Trans. Appl. Supercond.* **24** 6001105
- [15] Devred A *et al* 2012 Status of ITER conductor development and production *IEEE Trans. Appl. Supercond.* **22** 4804909
- [16] Bruzzone P L *et al* 2002 Upgrade of operating range for SULTAN test facility *IEEE Trans. Appl. Supercond.* **12** 520–3
- [17] Devred A *et al* 2014 Challenges and status of ITER conductor production *Supercond. Sci. Technol.* **27** 044001
- [18] Breschi M *et al* 2012 Results of the TF conductor performance qualification samples for the ITER project *Supercond. Sci. Technol.* **25** 095004
- [19] Seiler E *et al* 2016 Hysteresis losses and effective $J_c(B)$ scaling law for ITER Nb₃Sn strands *IEEE Trans. Appl. Supercond.* **26** 8200307
- [20] Abdyukhanov I M *et al* 2012 The RRR parameter of the ITER type bronze-route- Cr-Coated Nb₃Sn strands after different heat treatments *IEEE Trans. Appl. Supercond.* **22** 4802804
- [21] Kim J *et al* 2008 Effects of Cr diffusion on RRR values of Cr-plated Nb₃Sn strands fabricated by internal-tin process *IEEE Trans. Appl. Supercond.* **18** 1043–6
- [22] Alknes P *et al* 2015 Degradation of the Cu residual resistivity ratio in Cr-plated composite Nb₃Sn wires *IEEE Trans. Appl. Supercond.* **25** 6001306
- [23] Yum B-J and Kim K-W 2011 A bibliography of the literature on process capability indices: 2000–2009 *Qual. Reliab. Eng. Int.* **27** 251–68
- [24] Jewell M C *et al* 2010 World-wide benchmarking of ITER Nb₃Sn strand test facilities *IEEE Trans. Appl. Supercond.* **20** 1500–3
- [25] Pong I *et al* 2014 Worldwide benchmarking of ITER internal tin Nb₃Sn and NbTi strands test facilities *IEEE Trans. Appl. Supercond.* **27** 4802606
- [26] Cooley L D *et al* 2005 Costs of high-field superconducting strands for particle accelerator magnets *Supercond. Sci. Technol.* **18** R51–65
- [27] 2009 Supply Contract between The European Joint Undertaking for ITER and the Development of Fusion Energy and Bruker EAS GmbH (F4E-2008-OPE-005-02 (MS-MG)), (http://sec.gov/Archives/edgar/data/1500106/000104746911000530/a2201653zex-10_18.htm)
- [28] Luvata Press 2009 ‘Luvata cements position as leading global superconductor specialist with third nuclear fusion win’, (<http://luvata.com/en/News-Room/Press-Releases/Luvata-cements-position-as-leading-global-superconductor-specialist-with-third-nuclear-fusion-win-a-26-million-contract-from-US-Dept-of-Energy>)